Effect of Gasdermin D on Pyroptosis In Mouse Macrophages

A Major Qualifying Project Report:

Submitted to the Faculty of
WORCESTER POLYTECHNIC INSTITUTE

In partial fulfillment of the requirements for the
Degree of Bachelor of Science
In Biochemistry

By

_____
Colleen O'Shea

UMass Medical School Advisor:
Doctor Egil Lien
Department of Infectious Disease

WPI Project Advisor Approval:

_____
Professor Arne Gericke

Date: _____
Approved: _____

Abstract

Gasdermin D (GSDMD) is a protein encoded by the GSDMD gene and is found in the epithelial tissue and immune cells of humans. GSDMD is known to be cleaved into two segments, the pore forming domain on the N-terminal and the repressor domain on the C-terminal, by inflammatory caspases 1, 4, 5, and 11. Various bacterial strains were used to infect mouse macrophages with and without the GSDMD gene. The quantified difference in cell death between the two groups emphasizes the role of the GSDMD protein in the pyroptosis pathway.

Table of Figures

Table of Tables

Acknowledgements

I would like to take this time to thank Doctor Egil Lien for welcoming me into his research lab at UMass Medical School with the Infectious Disease department. He was a huge help in guiding me through understanding the importance of researching infectious pathogens. I would also like to thank Pontus Orning for his help teaching me lab techniques and how to culture cells. Without his help, I would still be wandering the lab looking for various supplies. I would also like to thank Doctor Arne Gericke for helping me find this MQP and helping me through the red tape and paperwork side of MQP. Thank you to everyone for your understanding and guidance through this project. I learned a lot about the biochemical side of infectious pathogens as well as a lot of skills to aid me in my future endeavors.

Chapter 1 - Introduction and Background

Gasdermin Superfamily

Gasdermins are a family of genes found in the epithelial tissue and mucous membranes of humans. This set of genes is highly specified to only a few types of epithelial cells. The human Gasdermin superfamily consists of GSDMA, GSDMB, GSDMC, GSDMD and related protein DFNA5 and DFNB59. The mouse Gasdermin superfamily consists of Gsdma1-3, Gsdmc1-4, and Gsdmd as well as the related protein Dfna5h and Dfnb59 (Tamura et al., 2007). The figure in Appendix A contains the exact chromosomal locations of each of the genes for both mice and human models. These genes are found in a variety of cell types in the body of both mice and humans. Table 1 below shows the locations of expression of each gene in the Gasdermin superfamily (Saeki & Sasaki, 2012).

Table 1: Gasdermin Superfamily Expression Sites (Saeki & Sasaki, 2012)

Gene Name [other name]	Mouse ortholog	Reported expression site in human (in mice)
Gasdermin Family genes		
GSDMA [Gasdermin (*GSDM*), Gasdermin1 (*GSDM1*)]	*Gsdma1, Gsdma2, Gsdma3*	Esophagus, stomach, skin, mammary gland
GSDMB [PRO2521 (*PRO2521*), Gasdermin-like (*GSDML*)]	(not identified)	Esophagus, stomach, liver, colon
GSDMC [Melanoma-derived leucine Zipper, extranuclear factor (*MLZE*)]	*Gsdmc1, Gsdmc2 Gsdmc3, Gsdmc4*	Esophagus, stomach, trachea, spleen, skin
GSDMD [Gasdermin domain-containing 1 (*GSDMDC1*), Dfna5-like (*DFNA5L*)]	*Gsdmd*	Esophagus , stomach
Gasdermin-related genes		
DFNA5	*Dfna5*	Placenta, brain, heart, kidney (cochlea)
DFNB59 [pejvakin]	*Dfnb59*	(Brain, eye, inner ear, heart, lung, kidney, etc)

All of the members of the Gasdermin Superfamily are expressed in the gastrointestinal tract of humans as well as other epithelial cells. Gasdermin A and Gasdermin C are expressed in the mature differentiated cell layer. Gasdermin B is expressed near stem cells, indicating that it may be tied to highly proliferating cells. Gasdermin D is mainly expressed in differentiating cells (Saeki & Sasaki, 2012). Although DFNA5 and DFNB59 have a conserved amino acid domain consistent with the other members of the Gasdermin family, the structures are not similar enough to have these genes included in the immediate family, thus leading them to be categorized in the Gasdermin superfamily instead(Tamura et al., 2007). Gasdermins are known to be involved in multiple types of cancers, but they are hypothesized to

act as tumor suppressors due to their heavy involvement in cell differentiation and regulation of pyroptosis (Aglietti & Dueber, 2017). A dominant mutation of DFNA5 has been found to be the cause of nonsyndromic hearing loss in humans (Ding et al., 2016).

Gasdermin D Structure

GSDMD was the gene of focus for the experiments conduced in this project. The protein that is encoded by Gasdermin D in humans is called hGSDMD, and the protein is called mGSDMD in mice. It is comprised of two distinct regions: the N-terminal pore forming domain (PFD) and the C-terminal repressor domain (RD). The space filling models of the entire molecule and the two separate domains is illustrated in Figure 1 below (Liu et al., 2018).

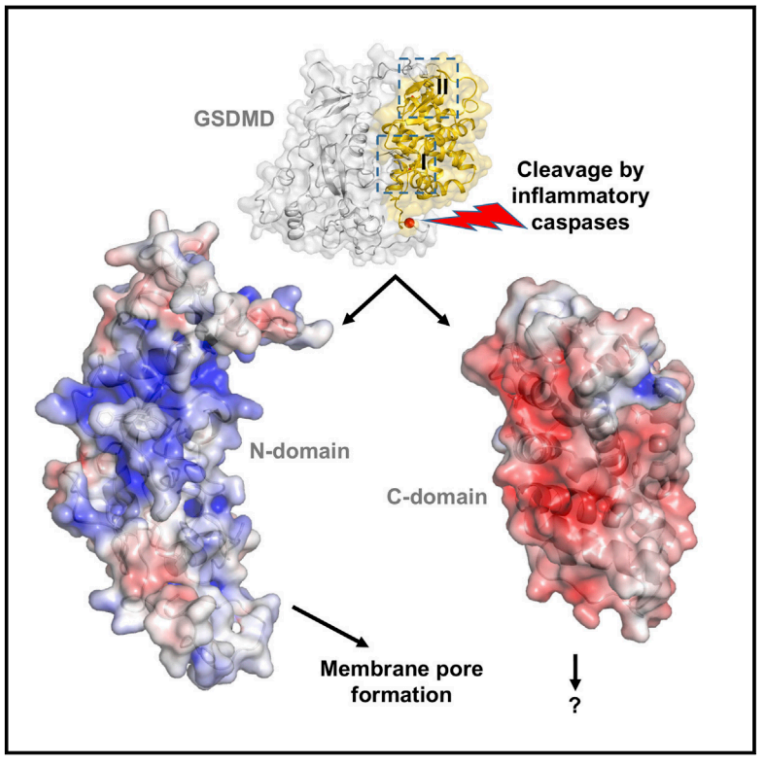

Figure 1: Molecular Structure of GSDMD (Liu et al., 2018)

The proposed interaction sites between the mGSDMD-C domain and the mGSDMD-N domain are illustrated in Appendix B. The first interaction site, box I, associates the α5, α8, and α12 helices on the c-domain and the α1 helix and the β1-β2 loop in the N-domain. The interaction between the domains also could possibly include the β11-α5 loop to additionally connect the two domains together. The second association site, box II, involves the C-domain α9 and α11 helices binding to the N-domain α4 helix. It was also found that the surface of the C-domain is only negatively charged at the N-domain interaction sites, where as the N-domain is mostly positively charged. This finding supports the theory that GSDMD-N has a role in binding to the phospholipid bilayer of the cell membrane (Ding et al., 2016; Liu et al., 2018).

DAMPs and PAMPs Effects on Adaptive Immunity

Pathogen-associated molecular pattern molecules (PAMPs) are specific molecular patterns in a pathogenic organism that are recognized by receptors in the cells involved in innate immunity. These receptor regions are called pattern recognition receptors (PRRs) and can commonly be found in macrophages, eosinophils and neutrophils in addition to natural killer cells, T-cells, B-cells and dendritic cells (Tang, Kang, Coyne, Zeh, & Lotze, 2012). PRRs also serve to alert the host immune system to invading pathogens and supports adaptive immunity. Another form of this pattern recognition is called damage-associated molecular pattern molecules (DAMPs). These signal to neighboring cells that there has been an unexpected cell death. This signal can result from damage to the cell, the invasion of the cell by a microbe, or any kind of stress that may cause cell death. DAMPs and PAMP's fill the extracellular space after an infection or the untimely death of a cell and initiate inflammatory response pathways (Lotze et al., 2007).

Interleukin-1β and Interleukin-18

Members of the IL-1 family, interleukin-1β and interleukin-18 are both pro-inflammatory cytokines that are vital for the successful immune response of the host organism. Pro-inflammatory cytokines induce an inflammatory immune response in the host organism. The symptoms of this include but are not limited to fever, localized swelling, cell death, and when it overwhelms the immune system it may cause severe sepsis which could lead to the death of the host organism (C A Dinarello, 2000b). In controlled levels, the organism will benefit from the inflammatory response, but an excess of pro-inflammatory cytokines leads to hyper-inflammation, negatively affecting the host organism. The inactive precursor of interleukin-1β (pro-interleukin-1β) is produced by the host cell in response to the presence of DAMPs and PAMPs. As a result, the host cell must encounter a second occurrence of a DAMP or PAMP in order to activate the interleukin-1β and initiate an inflammatory response (Lopez-Castejon & Brough, 2011). The interlukin-18 precursor, unlike interleukin-1β precursor, is always present even in healthy cells. This cytokine is similarly activated by inflammatory response precursors. IL-18 is directly activated by caspase-1 and is secreted by the cell in order to induce an inflammatory immune response (C A Dinarello, 2000a; Charles A. Dinarello, Novick, Kim, & Kaplanski, 2013).

Caspase-Mediated Inflammatory Response

Caspases are a category of enzymes that are important in regulating inflammatory response and cell death. Caspases exist in the cell in their inactive monomeric form and in order to become activated, some must be assembled into dimers or cleaved by precursor caspases. Caspase-1 is involved in regulating innate immune response and inflammation activity by releasing mature IL-1β. When caspase-1 is activated by the presence of a bacterium containing a specific molecular pattern**,** it cleaves pro-interleukine-1β into the activated form of IL-1β. This then initiates the secretion of these cytokines by the cell and causes an inflammatory response in the surrounding tissue (McIlwain, Berger, & Mak, 2013). Caspase-1 is recruited by canonical inflammasome complexes created in the cell in response to

PAMPs or DAMPs(Kayagaki et al., 2011). This inflammasome is then activated by pattern recognition receptors (PRRs) for PAMPs and DAMPs. Inflammasomes are comprised of one or two types of nod-like receptors (NLRs) at a time (Guo, Callaway, & Ting, 2015). These NLRs are activated by a wide variety of antagonists to the cell, and upon activation by the stimulus they cleave pro-caspase-1 into the active form of caspase-1 (Fukata, Vamadevan, & Abreu, 2009).

Human caspases -4 and -5 have the homologue caspase-11 in the mouse model. These caspases induce cytotoxicity in the host cell and ultimately leads to pyroptosis of the cell. This type of inflammation response is called non-canonical because it bypasses the canonical inflammasome pathway. This inflammatory response only requires LPS and pro-caspase -4, -5, or -11 to activate the caspases and initiate an inflammatory response in the cell. The resulting pyroptosis floods the extracellular space with IL-1β and IL-18, therefore initiating an inflammatory response from the surrounding uninfected cells (Yi, 2017). The distinction between canonical and non-canonical inflammasome pathways is illustrated in Figure 2 below.

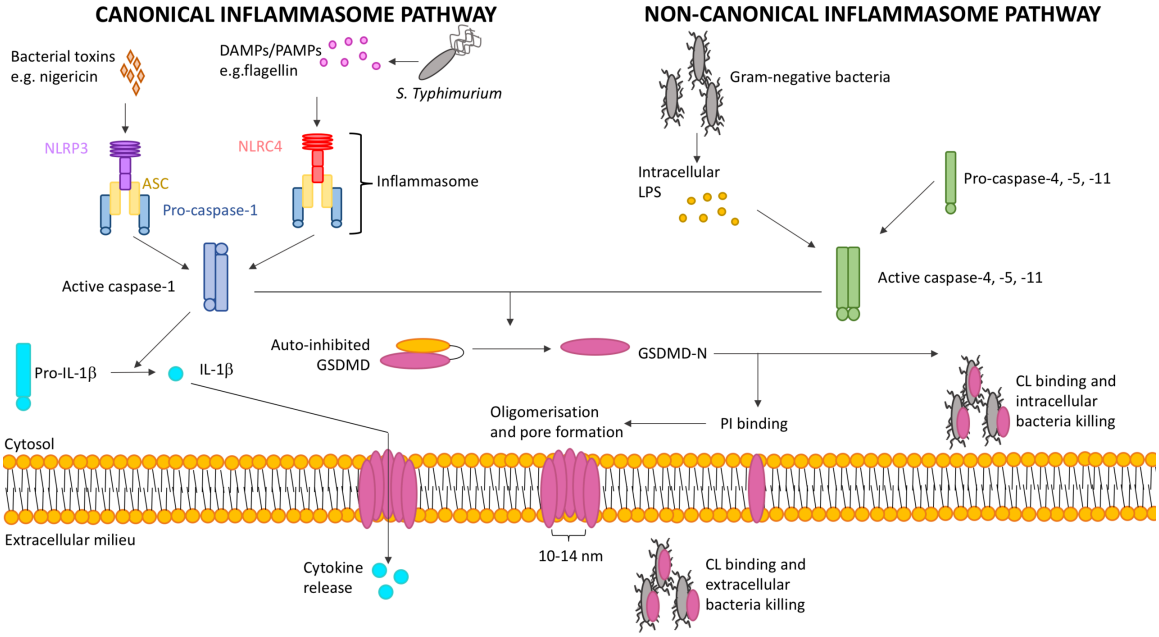

Figure 2: By Nataliechui619 - Own work, CC BY-SA 4.0, https://commons.wikimedia.org/w/index.php?curid=67261834

When a gram-negative bacterium infects a healthy cell, receptors in the cytosol of the cell detect the cytoplasmic lipopolysaccharide (LPS) embedded in the outer membrane of bacterium. The exact mechanism of action of how LPS is detected by caspase-11 is unknown (Shi et al., 2014). Once the LPS is bound by pro-caspase-11 in the cytosol, this complex then interacts with GSDMD. The Gasdermin D repressor domain is cleaved from the pore forming domain, and the pore forming domain is allowed to create a pore in the host cell membrane. This collective process is illustrated in Figure 2 above.

Role of GSDMD in Bacterial Infection

When a macrophage is infected with a bacterial pathogen according to the previous section, caspase-1, -4, -5, and -11 cleave Gasdermin D to separate the molecule into two domains. Once the repressor domain is cleaved from the pore-forming domain, the cytotoxic properties of GSDMD are initiated. The C-terminal repressor domain remains cytosolic while the N-terminal pore forming domain aggregates in the cell membrane in order to create a pore. This process can be visualized in Figure 3 below that I have created to visually simplify the pathway.

The pore becomes a location where inflammatory caspases escape the cell and the proton gradient is disrupted. Water and extracellular particles enter the cell and cause swelling of the until the membrane ruptures. This method of cell death is called pyroptosis because it is dependent on activation by caspase-1(Bergsbaken, Fink, & Cookson, 2009).

Apoptosis is a similar cell-mediated death resulting from an old, infected, or damaged cell, but does not produce an inflammatory response. The cell shrinks, the membrane blebs and a variety of caspases initiate this, meaning that apoptosis is not dependent on a single type of caspase for activation. Cytochrome c leaves the cell and binds to apoptotic protease activating factor (apaf-1). This then binds to pro-caspase-9 to create an apoptosome. This then cleaves the pro-caspase-9 to make the active form of caspase-9 which effects caspase-3, thus activating caspase-1. The caspases cascade is initiated from this initial caspase activation and it requires a variety of caspase-initiated reactions to complete apoptosis of the entire cell (Bergsbaken et al., 2009; Logue & Martin, 2008).

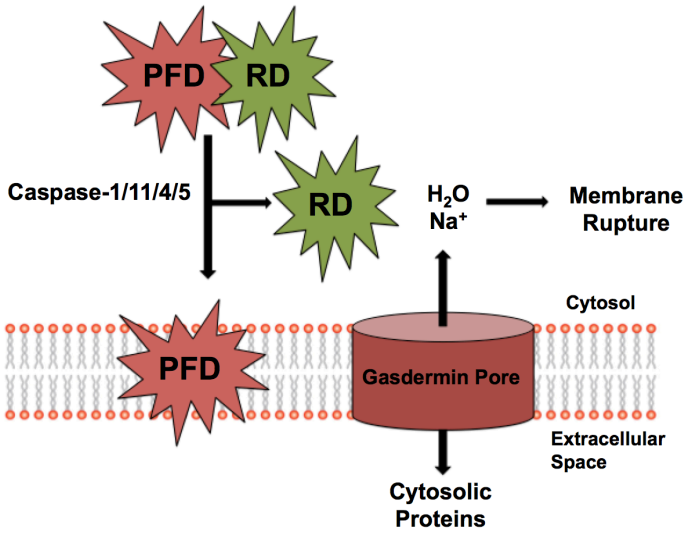

Figure 3: GSDMD

Once the pore in the membrane is large enough, extracellular components are able to enter the cell and disrupt the ion gradient between the cell and extracellular space. This is caused by water and ions entering the cell, leading to cell expansion and eventually the membrane is torn from the pressure and the cell dies.

In addition to outside species entering the cell, cytosolic proteins are now able to exit the cell. Some of these cytosolic proteins are the pro-inflammatory cytokines IL-1β and IL-18; which go on to initiate an immune response in the host organism (C A Dinarello, 2000a; Lopez-Castejon & Brough, 2011). The rupture of the cell membrane also floods the intracellular space with the contents of the infected cell. The cytokines released by the apoptotic cell signal the neighboring cells to initiate an inflammatory immune response. This response initiates caspases to cleave GSDMD and create an inflammatory response of their own. Because GSDMD and other Gasdermins are found in epithelial cells and mucous membranes, this inflammatory response is usually localized to those tissues. The inflammation can cause skin rashes, gastric pain and inflammation, nausea, and high fevers (C A Dinarello, 2000b).

Pyroptosis and apoptosis aid organism survival by recruiting immune response cells to the site of infection or injury. It may seem counterproductive for a cell to create a strong inflammatory response when a cell dies unexpectedly, but it is important for adaptive immunity in organism development. Apoptosis is important to cull the unhealthy cells from the host in order to ensure the damaged cell does not affect the neighboring healthy cells. DNA damage, injury, cytotoxicity, and infection are all reasons for apoptosis and pyroptosis to be initiated (Bergsbaken et al., 2009; Renehan, Booth, & Potten, 2001). Apoptosis has also been found to be vital for normal fetal development. Cells that comprise the nervous system and the immune system develop because of apoptosis from cells that do not create successful neuron connections or from cells that fail to produce antibodies. A healthy adult also initiates apoptosis of cells to regulate the number of viable cells in the organism and to prevent uncontrolled and unsustainable growth as well as replication of damaged DNA (Renehan et al., 2001).

Salmonella Enterica Infection

Salmonella enterica is an intracellular pathogenic bacterium that invades host cells via ingestion of contaminated food or water sources. The *Salmonella* aggregates in the intestinal epithelium of the host organism and initiates phagocytosis in these cells. Once the bacterium has entered the extracellular space surrounding the host cell, the PRRs and TLRs on the surface of the host cell membrane recognize characteristic parts of the bacterium. The flagellum on the *Salmonella* bacteria is one of the recognized patterns (Fukata et al., 2009; Ly & Casanova, 2007).

In order to avoid immune detection, the *Salmonella* bacteria creates a *Salmonella* containing vacuole (SCV) so that it can avoid direct immune detection by the cell. This allows the bacterium to enter the cells and have an environment suitable for proliferation ("Intracellular Infection by Salmonella | HHMI BioInteractive," n.d.; Ly & Casanova, 2007). *Salmonella* is incredibly virulent as a result of this pathogen's use of a type III secretion system (T3SS). These secretion systems allow gram-negative pathogenic bacteria like *Salmonella* and *Shigella* to bypass the defense systems in the cell membrane and directly inject bacterial effector proteins into the cytosol of the host cell (Coburn, Sekirov, & Finlay, 2007). These effector proteins change the environment of the host cell to make the

conditions perfect for the bacterium adhered to the surface of the outer cell membrane to invade the cell safely and proliferate effectively.

When the cell begins producing antimicrobial components such as cytokines to combat the change in homeostasis of the cell, the *Salmonella* bacteria can recognize this change and then responds by up regulating the virulence factors to combat the host cell defense mechanism. This allows the *Salmonella* to remain in the SVC and avoid detection longer (Broz, Ohlson, & Monack, 2012).

In this experiment, *Salmonella* mutants were used that had a profound effect on the virulence of the bacteria. The first gene mutation of *Salmonella*, ΔHilA, directly affects the host cell invasion mechanism. HilA is vital for initiating the invasion response of the *Salmonella* bacteria when in close proximity to host cells. This mutation removed the HilA gene so that the bacterium now has a reduced ability to invade host cells (Boddicker, Knosp, & Jones, 2003). The second mutation is on the ΔFlhD gene. This gene is responsible for the operation of the bacterial flagella. The flagella is important for the locomotion of the bacteria as well as initiating an immune response from recognition by NRLs and PRRs. Without this gene, flagella function is extremely limited and the NLR activation also will decrease substantially (Wang et al., 2016). Both of these mutations are expected to decrease rates of apoptosis in host cells.

Yersinia Pestis Infection

Yersinia pestis is a gram-negative pathogenic bacterium that is found all across the globe in host animals such as rodents and fleas. It is responsible for the bubonic plague, also known as the Black Death, which occurred in the mid-1300s and killed half of the population of Europe. *Yersinia pestis* is also classified as a category A bioterrorism agent. Although the plague is popularly thought to be a bacteria that does not effect today's population, the World Health Organization (WHO) has reported that between the years of 2010 to 2015 there were a total of 3248 reported cases of *Yersinia pestis*. Additionally, the most recent outbreak in Madagascar reported 2348 potential cases between August and November of 2017 ("WHO | Plague – Madagascar," 2017).

Yersinia pestis is similar to *Salmonella* in their infection mechanisms. *Yersinia pestis* invades the innate immune activity of the host organism by utilizing a T3SS like *Salmonella*. This secretion system is made up of a variety of proteins, and the outer proteins are collectively called Yops. These proteins are responsible for the interaction of the bacteria to the eukaryotic cell membrane of the host cells. Other Yops are integral in the transport of the effector molecules from the bacteria into the cytoplasm of the host cell (Bi et al., 2009; Li & Yang, 2008a). YopM is integral in the ability of *Yersinia pestis* to avoid activation of an immune response when the bacteria invades the cell.

YopM directly binds to caspase-1 and renders it incapable of initiating pyroptosis. Because pyroptosis is caspase-1 dependent, YopM effectively prevents the death of the cell and the release of inflammatory cytokines. This allows the *Yersinia pestis* to evade detection and replicate secretly within the host cell (LaRock & Cookson, 2012). The deletion of the gene that codes for this protein would cause the presence of *Yersinia pestis* in the host cell to activate a caspase-1 response and

initiate pyroptosis. The pyroptosis would create an inflammatory response at the infection site and the immune system of the host would be recruited to stop the spread of infection, thus lowering the virulence of the bacteria.

In this lab a different secretion system protein, YopJ, was studied in the infection experiments. YopJ is coded by the gene YpkA and is involved in initiating apoptosis of macrophages (Schoberle, Chung, McPhee, Bogin, & Bliska, 2016). YopJ negatively impacts the production of inflammatory caspases in the host cell. YopJ is the only Yop effector protein that induces apoptosis in the host cell and suppresses tumor necrosis factors (Lemaître, Sebbane, Long, & Hinnebusch, 2006). This means that *Yersinia pestis* now has significant influence over when the cell can induce apoptosis. *Yersinia pestis* needs this ability to be virulent because if the cell induces apoptosis too early in the infection, the *Yersinia pestis* no longer has a safe environment to replicate and will likely be attacked by the immune system. If *Yersinia pestis* can prevent the death of its host cell, it can replicate safely and induce apoptosis when the mature pathogenic bacteria are ready to spread to other cells in the host organism. A *Yersinia pestis* mutant was used in this experiment with a deficiency in Yopj. This mutation is expected to severely impact the virulence of the bacteria. The infected cells are expected to induce apoptosis to limit the spread of the mature bacteria.

2 - Materials and Methods

2.1 Mammalian Cell Culture

C57Bl/6 Cas9 BMDM (bone-marrow derived macrophages from mice) cells were immortalized by Pontus Orning, a member of the lab, using a J2 retrovirus expressing v-raf and v-myc oncogenes. These are considered the immortalized wildtype macrophages. Additionally, Pontus used lentivirally delivered specific gRNA to generate the GSDMD knock-out cells (CRISPR-Cas9 technology). The cells were then verified for the gene knock-out by use of GSDMD specific antibody (Genentech). Aliquots of these cells were collected from -80°F storage. They were placed on dry ice, and when in the hood they were partially thawed then transferred to a 50mL conical tube containing 10mL of DPBS. The cells were then placed into the centrifuge and spun for 5min at 4,000rpm in order to remove the DMSO before it caused harm to the cells. The supernatant was decanted and the pellet was resuspended by gentle pipetting in 10mL of serum-free cell culture media (DMEM). The cell solution was removed and transferred to a 75cm cell culture flask. The cells were then incubated at 37°C with daily media changes until they reached confluency. At this point the cells were split. This was done by aspirating the cell media over the entirety of the flask until no visible colonies of cells remained adherent to the bottom. The media was collected into a 50mL conical tube and centrifuged. The pellet was resuspended in cell media and only a fraction was replaced into the flask. Cell culture media was then added to the flask to ensure a thorough covering of the bottom of the flask when it is laid on its side. Cell concentration was determined by manually counting the number of viable cells using 40uL of Tryptan Blue dye and 40uL of the cell suspension. 10uL of this mixture was pipetted onto a glass slide and the viable cells

were counted using a microscope. This number was then multiplied by 2 to account for the 1:2 dilution of the sample with Tryptan Blue and then again multiplied by 10,000 to account for the size of the microscope slide and the total volume of the solution. The resulting number is the amount of cells per milliliter.

2.2 Bacterial Cell Culture

Salmonella enterica serovar Typhimurium, strain SL1344 and *Yersinia pestis* strain KIM5 in addition to the mutants discussed about were cultured fresh before every experiment. In order to do this, the frozen bacterial stocks were collected from -80°C storage and placed immediately on dry ice. The appropriate culture medium for the types of bacteria was determined and the culture plates were collected form the large walk-in refrigerator. A member of the lab had poured them at a previous time.

The micro centrifuge tubes containing the frozen bacterium were scraped with a cell scraper and the frozen bacterial solution was spread evenly on the appropriate plate for culture. TB agar was used for *Y. pestis* and LB agar was used for *Salmonella.* These plates were then put into either 37°C (*Salmonella*) or 26°C (*Yersinia Pestis*) incubators overnight. Once colonies were visible, the plates were stored in the refrigerator to stall their growth and save for future use. On the day of the infection procedure, a pipette tip was used to scrape colonies off of the plates and into 50mL of the appropriate liquid culture in a loose-topped vial. The bacterial solutions were placed into the appropriate incubation temperatures for their species. An hour before the infection, the *Yersinia Pestis* vials were moved to the 37°C incubator to jump-start the infectious state before adding the bacteria to the cell plate.

Cell concentration in the culture media was determined by measuring the absorbance of the bacterial samples in disposable cuvettes using a small bench top spectrophotometer. The samples were diluted with 1x PBS. The spectrophotometer was blanked with the PBS sample without bacteria and then the absorbance of the bacterial samples was measured at 600nm. This was then used to calculate how many colony-forming units (CFUs) were in each milliliter of the cell suspension.

2.3 Bacterial infection

The day before the bacterial infection, flat-bottomed 96-well cell culture plates were plated with 100,000 cells per well. The wells were planned out so that each different type of sample was plated in triplicate. The wells were filled with 200uL of DMEM cell culture media without FBS and the plate was incubated at 37°C overnight. In the morning, the media was aspirated off and replaced with new media. The wells were then infected with 1million bacterial cells/well of the bacterial strains selected. This as done by adding a small volume of the liquid bacterial cell culture to a volume of DMEM cell media to allow for 1 million bacterial cells to be transferred in 200uL. The cell media was aspirated from the plate and 200uL of the bacteria containing media was added to each well in accordance to the plate map. The plate was then placed in the designated bacterial infection incubator for 2-5 hours at 37°C. The length of time the cells incubated for was determined by the specific experimental protocol being followed. Experiments were conducted for

different time points to determine the difference in total cell death over time for each of the bacterial strains. After the bacterial infection was complete and the LDH samples were collected, 100uL of supernatant was collected from each well and placed into a plastic storage 96-well plate. This was covered with an adhesive plastic cover and stored in the freezer until the ELISA was ready to be conducted.

2.4 Lactate Dehydrogenase Cytotoxicity Assay

This assay was conducted using the Pierce LDH Cytotoxicity Assay Kit from Thermofisher Scientific (Part Number: 88953). This assay is used to quantifiably measure the level of cytotoxicity in cell samples. This was chosen because the experiments are designed to compare the level of cell death based on the bacteria the samples are infected with. This assay was conducted immediately after the bacterial infection of the samples was completed. 30 minutes before the end of the incubation in chapter 2.3, 10uL of the 10x Lysis Buffer from the LDH assay kit was added to the triplicate lysis control wells. This was done to provide a sample of a well that had a population of cells that were all theoretically dead. In addition to this control, three wells containing uninfected cell samples were used as the non-treated control wells. These wells theoretically display only cell death due to natural causes instead of bacterial infection. Three wells were also plated to be the LDH reagent blank wells. These wells did not contain cells, and only contained the LDH reagents in order to be able to remove their interference from the final absorbance readings. Once the infection was complete and the lysis buffer has incubated for at least 30 minutes, 50uL of each sample was transferred to a clean 96-well flat-bottomed plate. It was ensured at each sample was plated in triplicate. This assay was conducted in the fume hood with all lights turned off to ensure proper substrate color development.

The LDH assay kit was removed from the freezer and the Reaction Mixture (0.6mL Assay buffer and the entire volume of the Substrate Mix reconstituted with11.4mL of ultrapure water) was allowed to thaw in a place out of any direct light. Once thawed, 50uL of Reaction Mixture was added to each well and the plate was covered with the lid and enclosed in aluminum foil. The Lysis control well contained 10uL less Reaction Mixture to ensure a total volume of 100uL in each well. The plate was allowed to stand untouched for 30 minutes or until a distinct yellow color was observed in the standard wells and across the plate. 50uL of the Stop Solution was then added to each well in order to inhibit the substrate reaction. Gentle tapping mixed the plate and all bubbles were removed from the surface of the samples. The plastic lid was replaced and the plate was again wrapped in aluminum foil to prevent any further development of the substrate color. The plate was read in a microplate spectrophotometer at 490nm in order to determine the absorbance values of each of the wells. The data was analyzed based on the level of absorbance of the samples in comparison to the lysis control well and the untreated control well. The lysis well was considered to be 100% cell death, while as the untreated well was considered to be the 0% cell death. This untreated well is intended to take normal cell death into account and the treated wells measure the induced cell death due to the bacterial infection. The sample wells had the absorbance of the control well subtracted from them.

2.5 Mouse Interlukine1-β ELISA

The day before the ELISA assay was conducted; an uncoated clear-bottomed 96-well plate was prepared by adhering the antibodies to the bottom of the plate. The ELISA was done to identify the concentration of interlukine1-β, so the mouse IL-1β reagent kit from Invitrogen was used (Mouse IL-1 beta Uncoated ELISA, part number: 88-7013). The procedure contained in the reagent kit was used to conduct the assay. The plate was filled using a multichannel pipette with 100uL/well of Capture Antibody diluted 1:250 in 1x Coating Buffer (PBS diluted 1:10 in deionized water). The plate was then covered with a disposable adhesive cover and incubated at 4°C overnight until the assay was ready to be conducted. Following this incubation period, the plate was placed into a plate-washing instrument and washed three times with Wash Buffer (1x PBS). The plate was removed from the instrument and tapped upside-down on top of a paper towel until no liquid remained. Each well was then filled with 200uL of 1x ELISA diluent (Diluent Concentrate diluted 1:5 in DI water) and the plate was left to incubate at room temperature for one hour.

During this incubation period, the standard reagents were prepared. The standards need to be prepared fresh before every ELISA and cannot be stored for later use. The lyophilized cakes of mouse IL-1β standard were reconstituted with deionized water to bring the final concentration to 1000pg/mL. Following this incubation, the plate was again washed in the plate washer and all excess liquid was blotted out. Carefully not making contact with the bottom of the wells, a standard curve of mouse IL-1β concentration was then prepared on the now coated plate. First, 100uL of 1x ELISA Diluent was added to each of the standard wells, excluding the first well. Into the first standard well, 200uL of the highest mouse IL-1β concentration was added. From this well, 100uL of the solution was pipetted and moved to the second well in the standard series. For a total of 8 standard wells, this serial dilution was conducted. The remaining 100uL of solution at the end of the dilution series was discarded. In the standard 'blank' well, only 100uL of the 1x ELISA Diluent was added. In the sample wells, 100uL of each sample was added and their positions were recorded in a plate map. Once the samples were loaded, the plate was covered and incubated at room temperature for two hours. During this incubation period, the Detection Antibody (Diluted Detection Antibody 1:250 in 1x ELISA Diluent) was prepared.

Once the incubation was complete, the plate was washed in the plate washer three times, and all excess liquid was blotted on a paper towel. Once all excess liquid was removed, 100uL of Detection Antibody was added to each well and the plate was covered and incubated at room temperature for one hour. During this incubation, the Avidin-HRP solution was prepared (250x Avidin-HRP Concentrate diluted 1:250 in 1x Antibody Diluent). Following the incubation, the plate was washed three times in the plate washer and excess liquid was removed. To each well, 100uL of the HRP enzyme solution was added and the plate was then incubated at room temperature for 30 minutes. The plate was then washed and the excess liquid was removed. 100uL of the 1x TMB Substrate Solution (Tetramethylbenzidine) was added to each well and the plate was let to sit undisturbed at room temperature for 15 minutes. 50uL of Stop Solution (1M H_3PO_4)

was added to each well. The plate was then placed into a microplate spectrophotometer and the absorbance was measured at 450nm.

Chapter 3 - Results and Discussion

The mouse macrophages were thawed and cultured according to the protocol in chapter 2.1. The cells were grown in a 37°C incubator with CO_2. The next day, the cells were assessed for viability and confluency. There were a sufficient number of cells, so the experiment moved on to the next step. The cells were harvested and washed and then plated in a 96-well plate. The plate was then placed in the same incubator for another night. The bacterial cultures were thawed and plated on the same day the cells were plated into the 96-well plate. The liquid culture bacteria strains were placed in the appropriate incubators overnight, which are illustrated in chapter 2.2. On the morning of the infection, the bacteria in the liquid culture was diluted 1:10 in culture media and allowed to incubate for an hour. After the hour, the Yersinia pestis strains were transferred to the 37°C incubator to amplify their virulence. The bacterial cultures were left for another two hours and then were analyzed. The absorbance data is shown in Table 2 below.

Table 2: Absorbance values of Bacterial Cultures

OD600	Absorbance
Kim5	1.636
Yop J	1.892
SL1334	1.839
HilA	0.841
FlhD	3.366

The absorbance values were then multiplied by the multiplicity of infection (MOI) of each type of bacteria. *Yersinia pestis* strains were multiplied by 4.4×10^8 and the *Salmonella* samples were multiplied by 7.6×10^8 in order to determine the colony forming units in one milliliter (CFU/mL) of each bacterial culture. The results of the calculation are shown in Table 3 below. Additionally, the volume of the stock bacterial cell culture to add to 5mL of DMEM mammalian cell culture media was calculated in microliters. This calculation was used to add the appropriate amount of bacterium to each well in the cell culture plate.

Table 3: Bacterial Concentration Calculations

Bacteria	CFU/mL in Eppendorf	CFU in 5mL	V(mL) to add to 5mL of DMEM	uL to add to 5mL of DMEM
Kim5	719840000	10000000	0.0694599	69.46
Yop J	832480000	10000000	0.0600615	60.06
SL1334	1397640000	2000000	0.0357746	35.77
HilA	639160000	2000000	0.0782277	78.23
FlhD	2558160000	2000000	0.0195453	19.55

The cell plate was aspirated of cell media and the bacteria-containing cell media was added to the appropriate wells. Uninfected DMEM was added to control and lysis wells. The cells were covered and incubated at 37°C for two hours. At this point, 10mg/mL of gentamycin was added to each of the bacteria containing wells to limit the growth of the bacterial cells. The plate was then incubated for and additional 4 hours to ensure maximum infection rates. 30min before the harvest, lysis buffer was added to the lysis wells to serve as a control for the LDH assay.

This experiment resulted in an LDH plate that had no signal. The cause of the blank plate was not discovered, but the experiment was repeated. All new cells were cultured and new cell media was used to eliminate possible sources of contamination. After repeating the infection, another LDH assay was performed following the procedure in chapter 2.4, and the results were collected into Table 4 below.

Table 4: LDH Assay Absorbance Data

	Wild Type			GSDMD		
Blank	0.1538	0.1587	0.1449	0.1722	0.1671	0.1834
Lysis	0.5249	0.5565	0.6534	0.6779	0.7106	0.764
Kim5	0.2336	0.2885	0.2516	0.2883	0.2414	0.2894
ΔYop J	0.2271	0.2278	0.2032	0.1725	0.1616	0.1719
SL1334	0.4572	0.573	0.5125	0.5643	0.4231	0.6232
SLΔFlhD	0.2182	0.2614	0.2392	0.2158	0.2125	0.1957
SLΔHilA	0.1799	0.2761	0.2405	0.2308	0.2832	0.2206

The raw data as then calculated to be representative of a percentage cell death of the total cells in the well. This was done by subtracting the average of the absorbance values of the blank wells from every other absorbance value in the table. The corrected absorbances were then divided by the average of the lysis control wells to determine the ratio of LDH found in the sample wells to the LDH concentration found in the lysis control wells. The lysis control was considered to be complete cell death and maximum LDH concentration. This is shown in Figure 5 below.

Table 5: LDH of Wildtype Macrophages vs LDH of GSDMD knockout Macrophages

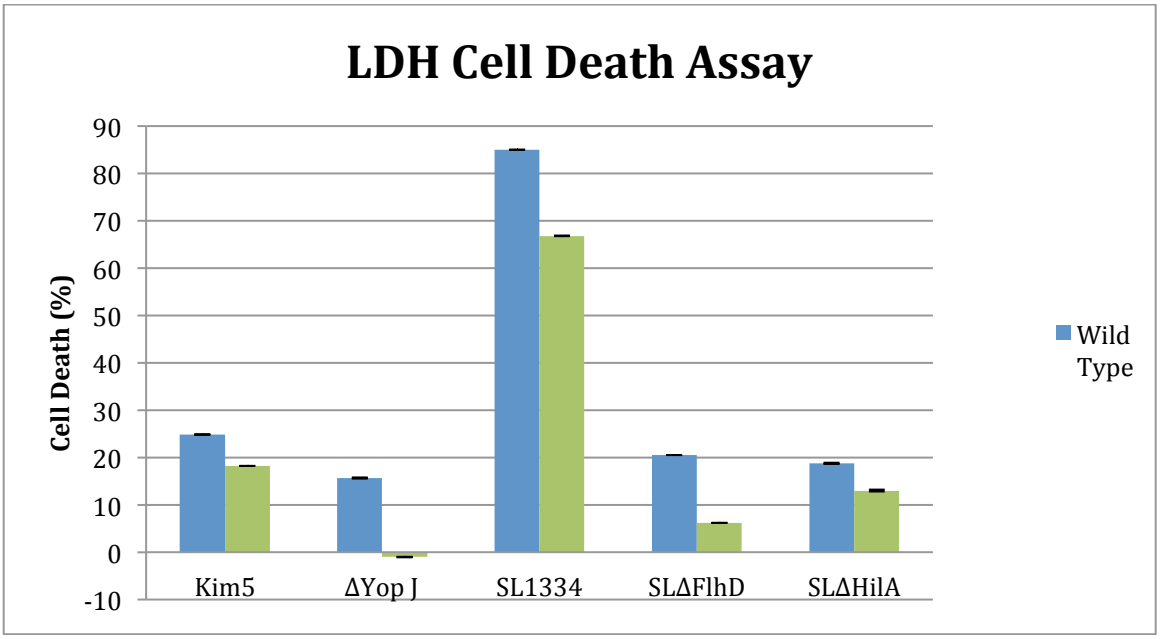

After the LDH assay was completed and the results were calculated, it was determined that the Kim5 sample, wildtype *Yersinia pestis*, did not have the LDH levels that were expected. The levels appear to be significantly lower than that of the *Salmonella* sample. It is undetermined if the source of contamination was completely eliminated in this repeat experiment, but it was decided that the plate could be used to conduct and ELISA assay because there may still be IL-1β present in the supernatant. The samples were collected and frozen overnight. The next day, the samples were thawed and the ELISA protocol was followed that is illustrated in chapter 2.5 to look for mouse IL-1β present in the samples. The standard curve was calculated from the absorbance of the standard samples added to the plate. This can be seen in Figure 4 below.

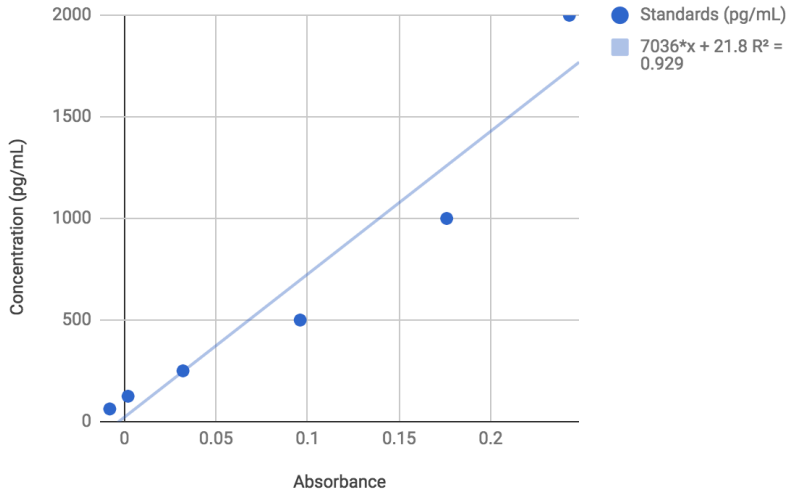

Figure 4: ELISA Standard Curve of Mouse IL-1 beta

After the standard curve was created, the IL-1 beta concentration of each of the samples could be calculated. This can be seen in Table 6 below.

Table 6: IL-1 beta Concentration Calculations

	CONCENTRATION (ng/mL)					
Control/ NT		-0.062632	0.190664		0.317312	-0.125956
Kim5	0.887228	0.718364	0.697256	0.570608	0.528392	0.275096
Yop J	1.858196	1.647116	1.224956	1.0772	0.718364	0.97166
SL1334	5.79132	7.19852	2.8362	5.15808	2.62512	2.69548
FlhD	5.50988	3.82124	3.11764	3.32872	1.99188	2.4844
HilA	4.17304	3.188	2.41404	2.20296	1.71044	1.49936

These concentrations in nanograms per milliliter were graphed to visually see the concentrations of IL-1 beta across all of the different samples. This can be seen in Figure 5 below.

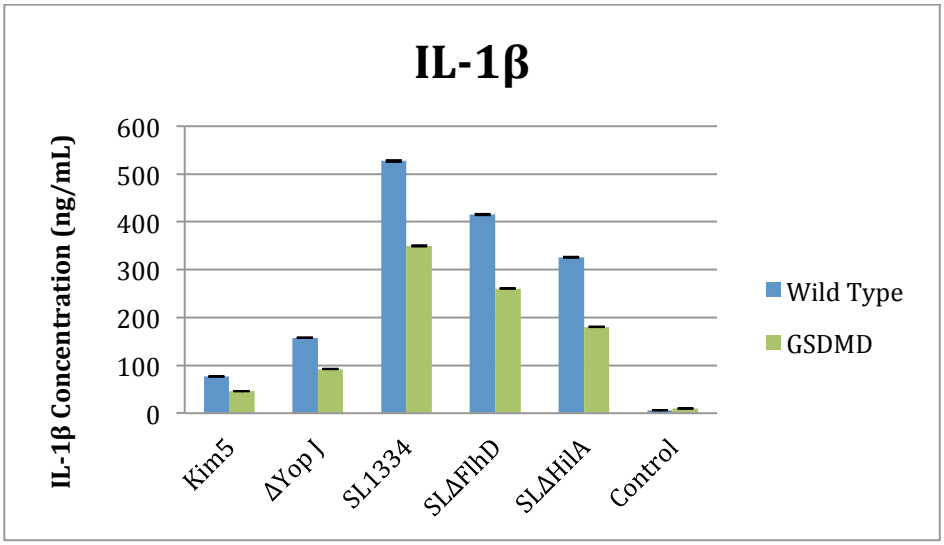

Figure 5: Mouse IL-1 beta Concentrations

Due to the results of the ELISA correlating with the LDH results, it was determined that the Kim5 bacteria samples were either contaminated or some external factor limited the virulence of the bacteria. The other bacterial mutations performed as expected. The mutations all caused a drop in the total cell death of the infected macrophages. This confirms that these specific mutations are integral to cell death regulation in the bacterium. This experiment was repeated again to determine better results, but the experiment collected incredibly poor data. There was some troubleshooting conducted again, but the problems were not resolved. A future MQP may wish to investigate why these infections did not produce the expected results.

References

Aglietti, R. A., & Dueber, E. C. (2017). Recent Insights into the Molecular Mechanisms Underlying Pyroptosis and Gasdermin Family Functions. *Trends in Immunology*, *38*(4), 261–271. https://doi.org/10.1016/j.it.2017.01.003

Bergsbaken, T., Fink, S. L., & Cookson, B. T. (2009). Pyroptosis: host cell death and inflammation. *Nature Reviews. Microbiology*, *7*(2), 99–109. https://doi.org/10.1038/nrmicro2070

Bi, Y., Du, Z., Han, Y., Guo, Z., Tan, Y., Zhu, Z., & Yang, R. (2009). Yersinia pestis and host macrophages: immunodeficiency of mouse macrophages induced by YscW. *Immunology*, *128*(1 Suppl), e406-17. https://doi.org/10.1111/j.1365-2567.2008.02990.x

Boddicker, J. D., Knosp, B. M., & Jones, B. D. (2003). Transcription of the Salmonella invasion gene activator, hilA, requires HilD activation in the absence of negative regulators. *Journal of Bacteriology*, *185*(2), 525–533. Retrieved from http://www.ncbi.nlm.nih.gov/pubmed/12511499

Broz, P., Ohlson, M. B., & Monack, D. M. (2012). Innate immune response to Salmonella typhimurium, a model enteric pathogen. *Gut Microbes*, *3*(2), 62–70. https://doi.org/10.4161/gmic.19141

Coburn, B., Sekirov, I., & Finlay, B. B. (2007). Type III secretion systems and disease. *Clinical Microbiology Reviews*, *20*(4), 535–549. https://doi.org/10.1128/CMR.00013-07

Dinarello, C. A. (2000a). Interleukin-18, a proinflammatory cytokine. *European Cytokine Network*, *11*(3), 483–486. Retrieved from http://www.ncbi.nlm.nih.gov/pubmed/11203186

Dinarello, C. A. (2000b). Proinflammatory cytokines. *Chest*, *118*(2), 503–508. Retrieved from http://www.ncbi.nlm.nih.gov/pubmed/10936147

Dinarello, C. A., Novick, D., Kim, S., & Kaplanski, G. (2013). Interleukin-18 and IL-18 Binding Protein. *Frontiers in Immunology*, *4*, 289. https://doi.org/10.3389/fimmu.2013.00289

Ding, J., Wang, K., Liu, W., She, Y., Sun, Q., Shi, J., … Shao, F. (2016). Pore-forming activity and structural autoinhibition of the gasdermin family. https://doi.org/10.1038/nature18590

Fukata, M., Vamadevan, A. S., & Abreu, M. T. (2009). Toll-like receptors (TLRs) and Nod-like receptors (NLRs) in inflammatory disorders. *Seminars in Immunology*, *21*(4), 242–253. https://doi.org/10.1016/j.smim.2009.06.005

Guo, H., Callaway, J. B., & Ting, J. P.-Y. (2015). Inflammasomes: mechanism of action, role in disease, and therapeutics. *Nature Medicine*, *21*(7), 677–687. https://doi.org/10.1038/nm.3893

Intracellular Infection by Salmonella | HHMI BioInteractive. (n.d.). Retrieved April 25, 2018, from http://www.hhmi.org/biointeractive/intracellular-infection-salmonella

Kayagaki, N., Warming, S., Lamkanfi, M., Walle, L. Vande, Louie, S., Dong, J., … Dixit, V. M. (2011). Non-canonical inflammasome activation targets caspase-11. *Nature*, *479*(7371), 117–121. https://doi.org/10.1038/nature10558

LaRock, C. N., & Cookson, B. T. (2012). The Yersinia virulence effector YopM binds caspase-1 to arrest inflammasome assembly and processing. *Cell Host & Microbe*, *12*(6), 799–805. https://doi.org/10.1016/j.chom.2012.10.020

Lemaître, N., Sebbane, F., Long, D., & Hinnebusch, B. J. (2006). Yersinia pestis YopJ suppresses tumor necrosis factor alpha induction and contributes to apoptosis of immune cells in the lymph node but is not required for virulence in a rat model of bubonic plague. *Infection and Immunity*, *74*(9), 5126–5131. https://doi.org/10.1128/IAI.00219-06

Li, B., & Yang, R. (2008a). Interaction between Yersinia pestis and the host immune system. *Infection and Immunity*, *76*(5), 1804–1811. https://doi.org/10.1128/IAI.01517-07

Li, B., & Yang, R. (2008b). Interaction between Yersinia pestis and the host immune system. *Infection and Immunity*, *76*(5), 1804–1811. https://doi.org/10.1128/IAI.01517-07

Liu, Z., Wang, C., Rathkey, J. K., Yang, J., Dubyak, G. R., Abbott, D. W., & Xiao, T. S. (2018). Structures of the Gasdermin D C-Terminal Domains Reveal Mechanisms of Autoinhibition. *Structure*. https://doi.org/10.1016/j.str.2018.03.002

Logue, S. E., & Martin, S. J. (2008). Caspase activation cascades in apoptosis. *Biochemical Society Transactions*, *36*(1), 1–9. https://doi.org/10.1042/BST0360001

Lopez-Castejon, G., & Brough, D. (2011). Understanding the mechanism of IL-1β secretion. *Cytokine & Growth Factor Reviews*, *22*(4), 189–195. https://doi.org/10.1016/j.cytogfr.2011.10.001

Lotze, M. T., Zeh, H. J., Rubartelli, A., Sparvero, L. J., Amoscato, A. A., Washburn, N. R., … Billiar, T. (2007). The grateful dead: damage-associated molecular pattern molecules and reduction/oxidation regulate immunity. *Immunological Reviews*, *220*(1), 60–81. https://doi.org/10.1111/j.1600-065X.2007.00579.x

Ly, K. T., & Casanova, J. E. (2007). Mechanisms of *Salmonella* entry into host cells. *Cellular Microbiology*, *9*(9), 2103–2111. https://doi.org/10.1111/j.1462-5822.2007.00992.x

McIlwain, D. R., Berger, T., & Mak, T. W. (2013). Caspase functions in cell death and disease. *Cold Spring Harbor Perspectives in Biology*, *5*(4), a008656. https://doi.org/10.1101/cshperspect.a008656

Renehan, A. G., Booth, C., & Potten, C. S. (2001). What is apoptosis, and why is it important? *BMJ (Clinical Research Ed.)*, *322*(7301), 1536–1538. Retrieved from http://www.ncbi.nlm.nih.gov/pubmed/11420279

Saeki, N., & Sasaki, H. (2012). Gasdermin Superfamily : A Novel Gene Family Functioning in Epithelial Cells. *Endothelium and Epithelium*, 193–211.

Schoberle, T. J., Chung, L. K., McPhee, J. B., Bogin, B., & Bliska, J. B. (2016). Uncovering an Important Role for YopJ in the Inhibition of Caspase-1 in Activated Macrophages and Promoting Yersinia pseudotuberculosis Virulence. *Infection and Immunity*, *84*(4), 1062–1072. https://doi.org/10.1128/IAI.00843-15

Shi, J., Zhao, Y., Wang, Y., Gao, W., Ding, J., Li, P., … Shao, F. (2014). Inflammatory caspases are innate immune receptors for intracellular LPS. *Nature*, *514*(7521), 187–192. https://doi.org/10.1038/nature13683

Tamura, M., Tanaka, S., Fujii, T., Aoki, A., Komiyama, H., Ezawa, K., … Shiroishi, T.

(2007). Members of a novel gene family, Gsdm, are expressed exclusively in the epithelium of the skin and gastrointestinal tract in a highly tissue-specific manner. *Genomics*, *89*(5), 618–629. https://doi.org/10.1016/J.YGENO.2007.01.003

Tang, D., Kang, R., Coyne, C. B., Zeh, H. J., & Lotze, M. T. (2012). PAMPs and DAMPs: signal 0s that spur autophagy and immunity. *Immunological Reviews*, *249*(1), 158–175. https://doi.org/10.1111/j.1600-065X.2012.01146.x

Wang, K.-C., Huang, C.-H., Ding, S.-M., Chen, C.-K., Fang, H.-W., Huang, M.-T., & Fang, S.-B. (2016). Role of yqiC in the Pathogenicity of Salmonella and Innate Immune Responses of Human Intestinal Epithelium. *Frontiers in Microbiology*, *7*, 1614. https://doi.org/10.3389/fmicb.2016.01614

WHO | Plague – Madagascar. (2017). *WHO*. Retrieved from http://www.who.int/csr/don/27-november-2017-plague-madagascar/en/

Yi, Y.-S. (2017). Caspase-11 non-canonical inflammasome: a critical sensor of intracellular lipopolysaccharide in macrophage-mediated inflammatory responses. *Immunology*, *152*(2), 207–217. https://doi.org/10.1111/imm.12787

Appendix

Appendix A: Chromosome Locations of Gasdermin Family Members (Tamura et al., 2007)

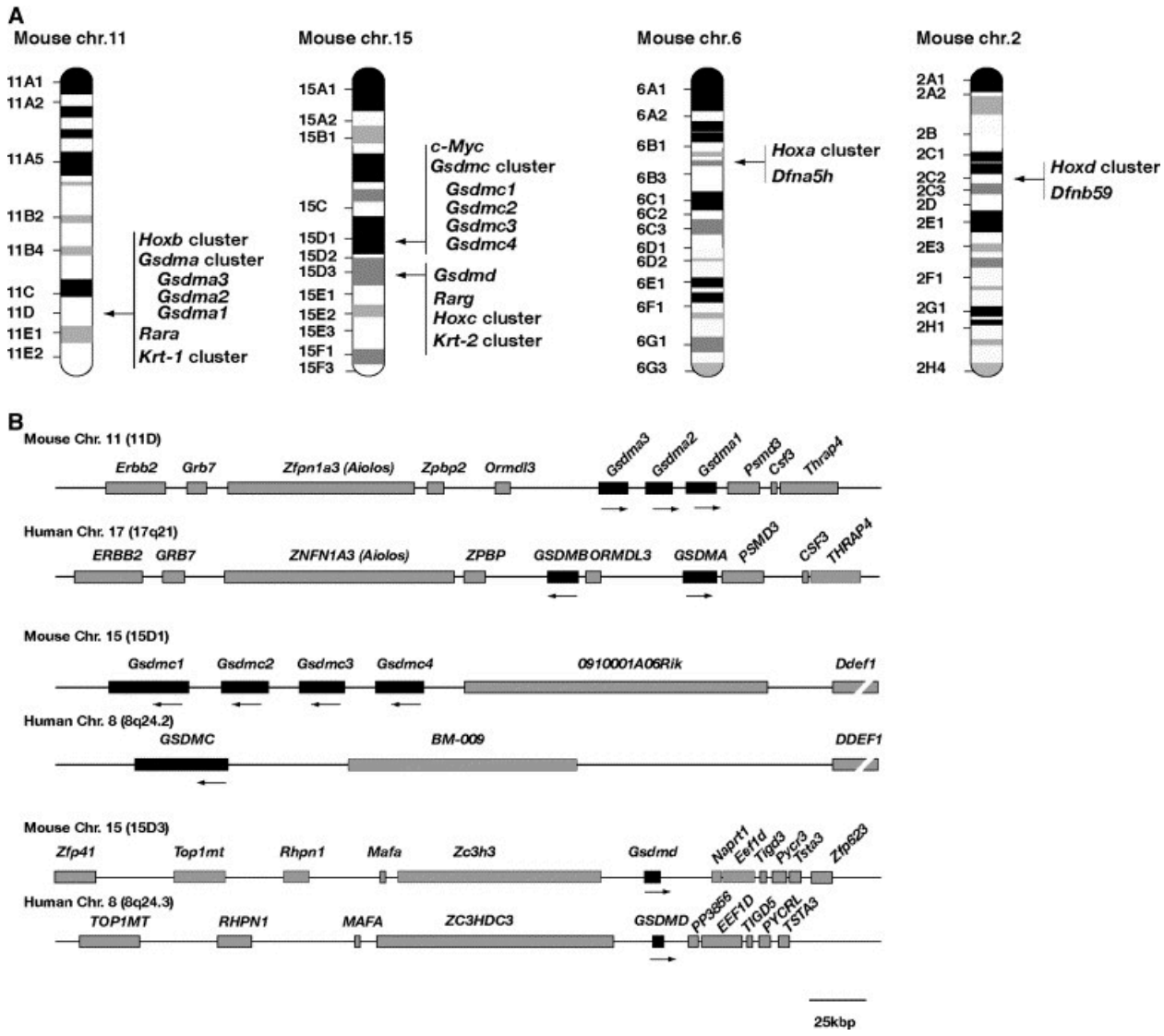

Appendix B: GSDMD Molecular Structure and Domain Interaction Sites

The complete molecular structures of GSDMD are modeled below. The sites where GSDMD-C and GSDMD-N interact are shown in the I and II labeled boxes (Liu et al., 2018).

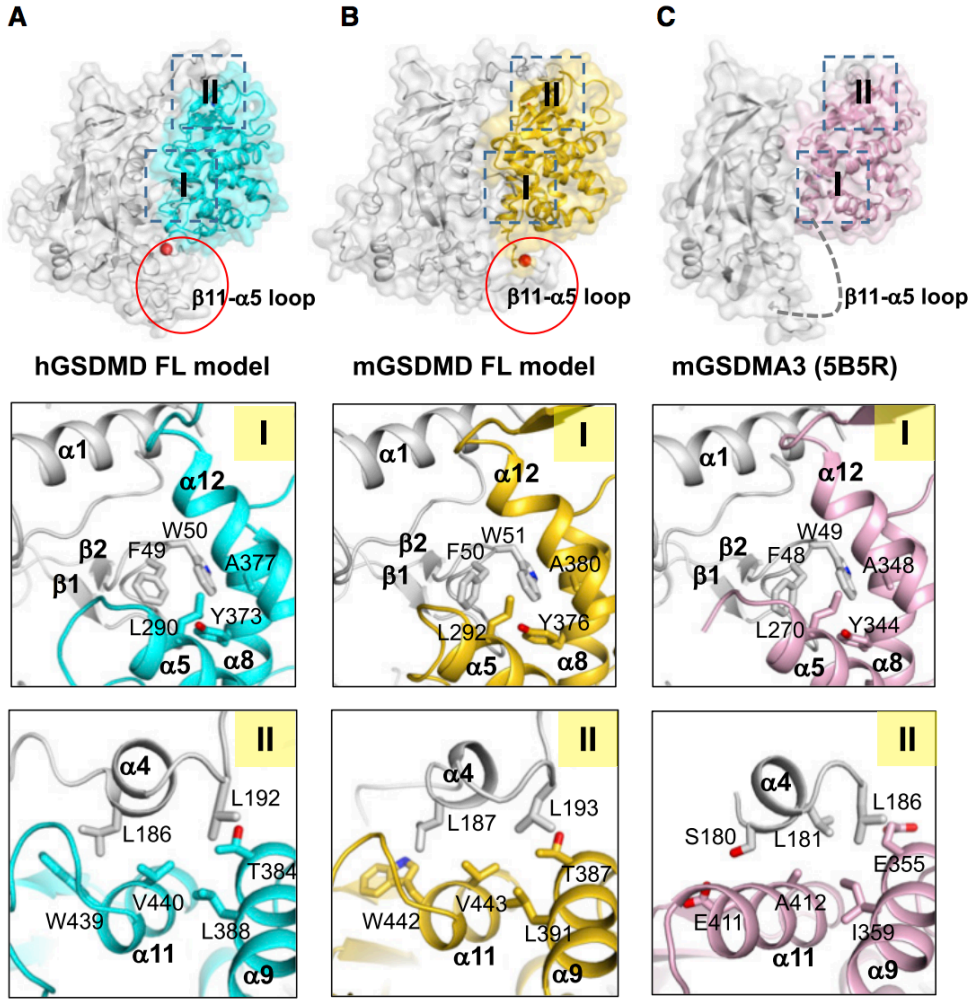

Figure 2. The N- and C-Domain Interface for hGSDMD, mGSDMD, and mGSDMA3

The full-length hGSDMD and mGSDMD structural models were created using the full-length mGSDMA3 as a template. The N and C domains of an hGSDMD model are shown as gray and cyan surface, respectively, in (A). The two domain interaction sites I and II are outlined in the top panel, with the details shown on the lower two panels as ribbons and sticks. Similar representations are shown for mGSDMD in (B) with the C domain colored gold, and mGSDMA3 in (C) with the C domain colored pink. The hGSDMD and mGSDMD caspase cleavage sites are shown as red spheres in (A) and (B), respectively. See also Figure S2.

Appendix C: Yersinia Pestis Infection via Flea Bite

Diagram of Yersinia pestis infection of host organism cell types (Li & Yang, 2008b).